Twin Model-based Fault Detection and Tolerance Approach for In-core Self-Powered Neutron Detectors*

Jing Chen,[1] Yan-Zhen Lu,[1] Hao Jiang,[1,†] Wei-Qing Lin,[1] and Yong Xu[2,3]

[1]*College of Electrical Engineering and Automation, Fuzhou University, Fuzhou 350108, China*
[2]*The Department of Automation, Shanghai Jiao Tong University, Shanghai 200240, China*
[3]*Fujian Fuqing Nuclear Power Co., Ltd., Fujian 350318, China*

The in-core self-powered neutron detector (SPND) acts as a key measuring device for the monitoring of parameters and evaluation of the operating conditions of nuclear reactors. Prompt detection and tolerance of faulty SPNDs are indispensable for reliable reactor management. To completely extract the correlated state information of SPNDs, we constructed a twin model based on a generalized regression neural network (GRNN) that represents the common relationships among overall signals. Faulty SPNDs were determined because of the functional concordance of the twin model and real monitoring systems, which calculated the error probability distribution between the model outputs and real values. Fault detection follows a tolerance phase to reinforce the stability of the twin model in the case of massive failures. A weighted K-nearest neighbor model was employed to reasonably reconstruct the values of the faulty signals and guarantee data purity. The experimental evaluation of the proposed method showed promising results, with excellent output consistency and high detection accuracy for both single- and multiple-point faulty SPNDs. For unexpected excessive failures, the proposed tolerance approach can efficiently repair fault behaviors and enhance the prediction performance of the twin model.

Keywords: Self-powered neutron detector, Twin model, Fault detection, Fault tolerance, Generalized regression neural network, Nuclear power plant

I. INTRODUCTION

Neutron flux is an important variable in nuclear reactors. Monitoring the variation and distribution of the neutron flux is essential to maintain the power stability of nuclear reactors [1]. At present, self-powered neutron detectors (SPNDs) are widely employed in core neutron flux measurement systems (CNFMS) of nuclear power plants (NPPs) to accurately measure neutron flux and provide highly reliable three-dimensional (3D) power distribution information. However, the risk of failure has increased with the increasing scale and complexity of the control of modern nuclear reactors[2].

Faulty SPNDs that either completely or partially fail provide incorrect monitoring information, which may negatively affect both the simple and more advanced functionalities of the system, resulting in degradation of the overall system performance and an increased risk level [3]. Techniques to address these problems can be classified as hardware redundancy methods, model-based methods, and data-driven methods [4, 5]. Generally, hardware redundancy measures in which more than three SPNDs are installed to observe the neutron flux within a range of space are employed for NPPs to improve the reliability of CNFMS. Assuming that any one SPND in a neutron measurement channel fails, the additional SPNDs still function and maintain high-accuracy measurements. Although this measure can prevent occasional intermittent failures from negatively affecting the system, the inability to implement fault tolerance can lead to false perceptions of the performance of the CNFMS when redundant SPNDs fail simultaneously. Moreover, redundant SPNDs continue to incur high installation and maintenance costs, which adversely affect the economics of NPPs [6].

Popular model-based methods (such as Kalman filtering [7], mixed Kullback–Leibler divergence and exponential weighted moving average [8], high-gain observer [9], the Monte Carlo method [10], and extended state observer [11]) handle fault detection using simple mathematical models that formulate fault signatures. The results of these methods for specific nonlinear systems have been developed under various restrictive assumptions. Recently, data-driven methods [12–14] have been used to perform fault detection for ker equipment in NPPs; the main principle is to establish an object model based on data analyses and realize accurate detection using model outputs with constraints of the evaluation criteria [15]. Peng *et al.* [3] constructed mathematical models for various detectors using principal component analysis (PCA) and achieved fault detection and isolation for SPNDs through the square prediction error of linear models and the detector validity index based on the reconstruction. Yellapu *et al.* [16] developed a method based on multiscale PCA with wavelet transform to reduce the modeling cost and improve the sensor fault diagnosis results by calculating the wavelet approximation coefficient. An online multiscale data reconciliation scheme for detecting and isolating sensor faults in advanced heavy-water reactors was proposed in [17]; the scheme achieved high accuracy under different scenarios. Li *et al.* [18] employed two different fault identification methods to locate faults more accurately. One was an improved weighted contribution analysis method based on the traditional contribution analysis of sensors to Q statistics. The second method was based on the sensor validity index obtained using the iterative reconstruction method. However, static linear models are typically unable to detect long-term SPND faults. To improve the detection efficiency of practical

* Supported by the Natural Science Foundation of Fujian Province, China (No. 2022J01566).
† Corresponding author, jiangh@fzu.edu.cn

time-varying faults, Chatterjee *et al.* [19] proposed the use of instantaneous cluster statistics to normalize the measurements of each SPND in clusters and update the PCA model using normalized values. This approach resulted in lower false alarm rates and higher detection rates for real-time fault changes than traditional static models. Experimental results show that these approaches are useful in identifying faulty instruments. Yu *et al.* [20] proposed improvements to the traditional PCA model through a new corrected reconstruction algorithm to reconstruct the principal component and the residual space. A cyclic PCA monitoring model was established to accurately detect different types of faults and reconstruct fault data. Nageswara *et al.* [21] performed information fusion by combining the ensemble of trees and the support vector machine (SVM) algorithm to evaluate the calculation error of multiple sensors and the influence of complementary and redundant sensors. Most studies have failed to focus on the inherent correlation among all SPND signals in the overall detector assemblies. For the dozens of SPNDs existing in neutron flux measurement channels, challenges in information integration and correlation analysis remain because of difficulties in handling large amounts of data simultaneously.

As a new enabling technology, a digital twin (DT) can act as a mirror of the real world by providing an integrated environment for simulating, decision-making, and optimizing physical system operations [22, 23]. Because of the powerful computing capabilities and cognitive intelligence of DT, developing more refined and scalable models for fault detection has become possible. Lin *et al.* [24] developed a nearly autonomous management and control (NAMAC) system for advanced nuclear reactors with DT technology. Cai *et al.* [25] proposed analytical techniques based on data and information fusion for modeling and developing DT virtual machine tools. DT applications in the context of NPPs have proliferated recently [26–28]. The development of DT combined with advanced technologies for detection, control, and optimization can significantly improve system performance, reliability, availability, maintainability, and operational flexibility. Therefore, efficient in-core SPND fault detection and the maintenance of monitoring systems using twin technologies are our major objectives. To continue such interesting exploration of research on SPND signals, a twin model using DT technology was constructed for the parameter analysis of an in-core nuclear reactor with large monitoring data and complex and changeable operating conditions. In this case, the established twin model can extract rich values from isolated time-varying data without disturbing the equipment on the real physical layer and can simulate the real-time state and dynamic characteristics of SPND entities through interactive data, overcoming the problem that traditional mathematical models [29] cannot effectively deduce the fault state of multidimensional signals in real time. In addition, several researchers have devoted their attention to state analysis and to the design of DT models of key nuclear reactor components. Hu *et al.* [30] comprehensively described the research status and development directions of DT technology in the field of advanced nuclear energy, proposed a multidimensional evaluation digital model suitable for application in nuclear reactors, and preliminarily established the fault diagnosis process. Wang *et al.* [31] proposed a DT system of the out-of-core detector assisted with an installation robot to perform real-time visualization monitoring of the detector installation and replacement process. Gong *et al.* [32] combined reduced-order models with machine learning to create physics-based DTs using parameters input in real time to rapidly reconstruct the neutron field in the core. Cancemi *et al.* [33] generated primary nuclear components through numerical simulation of different plant conditions, which may support the predictive maintenance optimization based on plant condition and the development of a DT model for improving plant safety and availability.

Because the implementation of the twin model significantly depends on the information transferred from valid data [34], the frequent and unexpected fault behaviors of SPNDs only provide unrepresentative data, leading to serious distortions in the outcomes and even the unprecedented collapse of the twin model. The decision made after calculations based on a large amount of incorrect information fails to realize the entire purpose of maintaining normal system function. Most recent research methods have focused on fault detection, and only a limited amount of research has been conducted to simultaneously achieve fault tolerance in critical detectors at NPPs. This is one of the principal motivations for this work. Designing a reasonable fault tolerance strategy that would work uninterruptedly with sufficient information-processing capabilities is practically challenging. Li *et al.* [35] suggested an active fault tolerance control method based on the improved BP neural network, which controls fault sensors by reconstruction. Kim *et al.* [36] developed a method of evaluating the fault detection coverage of a fault-tolerant technique using a fault injection experiment in a safety-critical digital I&C system for NPPs. They also proposed a probabilistic safety assessment model to observe the effect of the fault detection coverage of fault-tolerant techniques. To enhance the stability of a modular high-temperature gas-cooled reactor system and the control rod drive mechanism, Hui *et al.* [37] proposed an adaptive fault-tolerant control scheme based on a radial basis function neural network, which has a higher load tracking accuracy and better fault tolerance to systems. Li *et al.* [38] proposed an active fault-tolerant control scheme based on the deep Q-network algorithm of reinforcement learning to maintain the stability of the once-through steam generator control system. Rangegowda *et al.* [39] introduced a fault tolerance control framework to arrest the performance degradation of conventional controllers in the presence of sensor bias. Clearly, appropriate fault tolerance operations are required to handle the incorrect information provided by failed equipment, which can ensure data purity and no interference for the normal performance of the twin model. Therefore, introducing an appropriate fault-tolerance strategy to SPND fault detection is advantageous to maintain a healthy interaction of data information and pave the way for reliable outputs of the twin model in the long term.

In this study, we propose an effective fault detection and

tolerance approach for in-core SPNDs based on a twin model. The SPNDs are uniformly distributed in the reactor core; a generalized regression neural network (GRNN) [40] is employed to construct the twin model, which is consistent with the real system and represents the common relationship between the overall signals. In this manner, the state correlation between the SPND signals is completely considered, and the output characteristics of specific SPND individuals can be described using the joint feature information of the surrounding SPNDs. Then, state analysis and fault detection of the SPNDs were realized by analyzing the probability distribution of errors between the outputs of the twin model and the real value. To achieve fault tolerance for unexpected faulty SPNDs, we useda weighted k-nearest neighbor (WKNN) [41] to recover and reconstruct faulty signals. Through troubleshooting, data substitution, and data verification of faulty SPNDs, the accuracy and rationality of the detection results can be significantly improved. Compared with the traditional single-signal analysis model, the proposed approach can detect multi-point faults more simply and efficiently.

The remainder of this paper is organized as follows: Section 2 provides a brief description of the measurement channel distribution of the neutron flux and the composition of the SPND. Section 3 describes the construction scheme of the twin model and the specific framework for fault detection and tolerance. The experimental results and discussion are presented in Section 4. Finally, the conclusions of the proposed framework are provided in Section 5.

II. BRIEF DESCRIPTION OF SPND

An in-core neutron instrument is one of the most important types of nuclear power equipment. SPNDs provide a crucial basis for neutron flux measurement for safe operation, treatment of abnormal working conditions, and post-accident monitoring of NPPs. In this study, an integrated core instrument casing assembly was used in a pressurized water reactor for third-generation NPPs. As shown in Fig. 1, the core contains 44 radially distributed measurement channels. In each channel, a core detector assembly that is installed in the instrument tube of the fuel assembly contains seven axially distributed SPNDs in equidistant layers.

SPNDs have been developed to meet the requirements of small size, long life, and high tolerance to harsh environments. The composition of SPNDs is shown in Fig. 2, which mainly consists of an emitter, an insulator, and a collector. The communication line is constructed using a two-core cable in the form of armor and measures the currents generated by the emitter and noise currents caused by the background core. The currents are then transmitted to the processing cabinets through the connector and transmission cable. Because the noise currents are very small, they can be ignored. Generally, rhodium SPNDs are used in pressurized water reactor NPPs. The main generation process of SPND currents is determined by the radiation capture reaction, which proceeds in the emitter material ${}_{45}Rh^{103}$ with the generation and subsequent disintegration of the induced beta-active isotope ${}_{45}Rh^{104}$. Then, the beta particles induced by disintegration escape from the emitter with a certain probability and are collected by the collector, leading to the emitter becoming positively charged. Thus, the currents are proportional to the neutron flux absorbed at the location of the SPND emitter in the reactor.

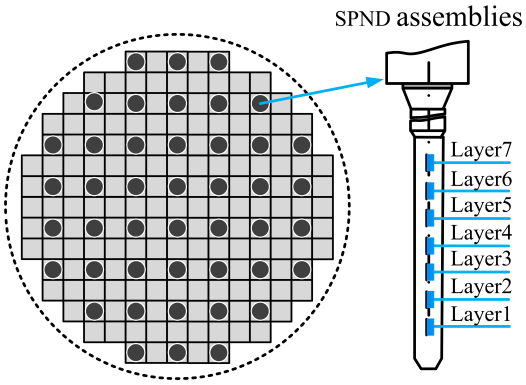

Fig. 1. Distribution of the neutron flux measurement channels

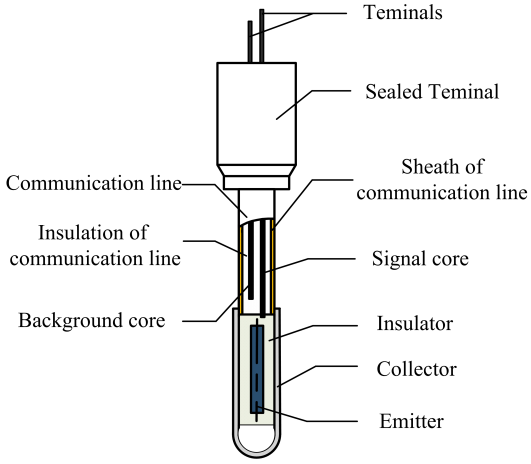

Fig. 2. Composition of SPND

III. METHODOLOGY

The purpose of this study is to use the twin model to enhance SPND detection performance. The main goal of the DT model is to create a mirror image of the physical entities in the digital realm by observing the data features and intrinsic correlation information among real SPND signals. In this study, we conducted a further state analysis of the current signals generated by radially distributed SPNDs on the plane of the reactor core of a specific NPP. As shown in Fig. 3, n SPNDs are uniformly arranged on the cross section of the in-core vessel. Each SPND is responsible for the neutron radiation capture reaction in the relevant space range, which results

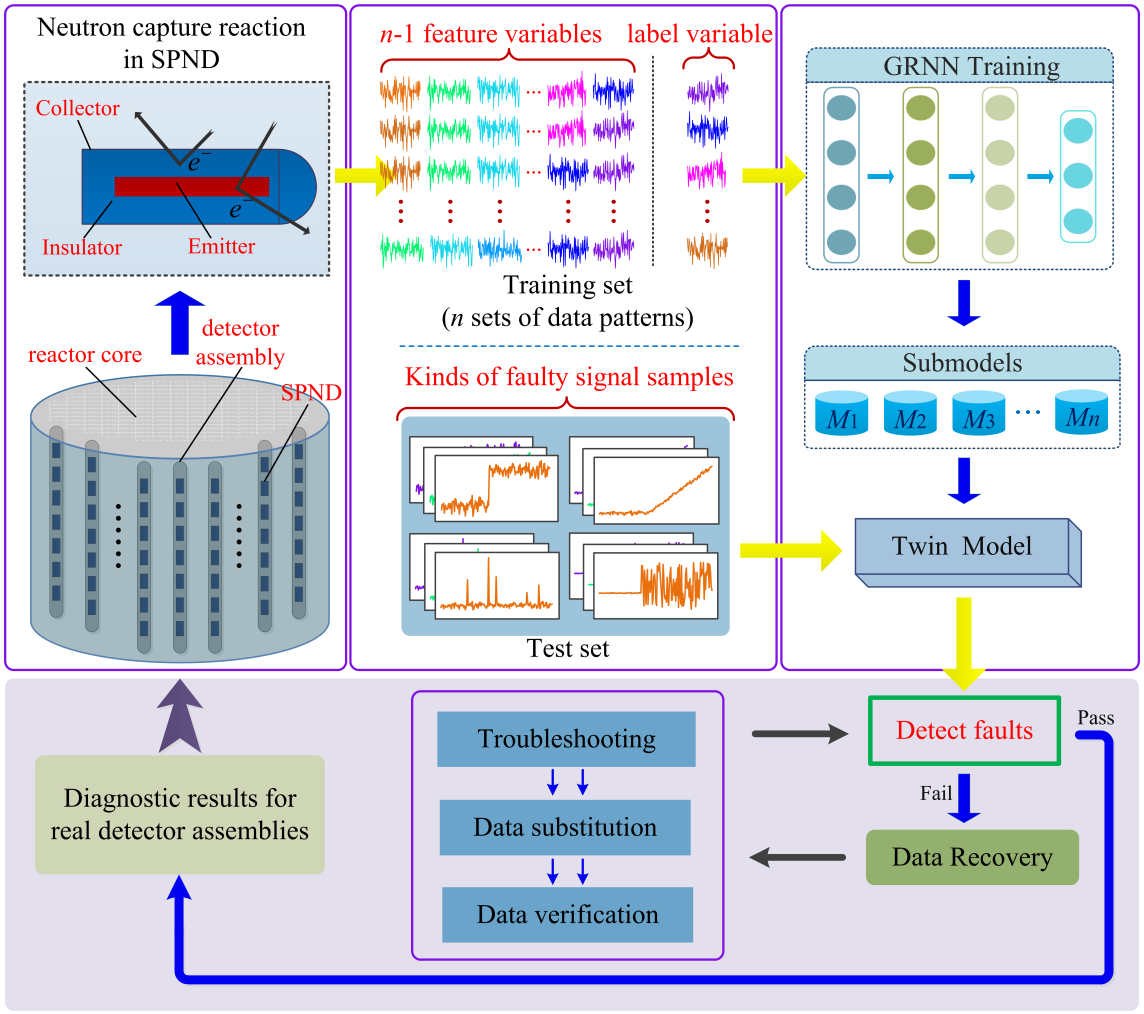

Fig. 3. The framework of the proposed SPND fault detection and tolerance method

in n groups of recorded current signals. Each data-twinning procedure for an SPND requires signal analysis of a particular SPND by observing the signal values of the other n-1 SPNDs. Therefore, the remaining n-1 SPND signals are used as model input characteristic variables, including a particular SPND label variable, prior to model training. We can obtain n sets of data patterns with related feature and label variables for each SPND. Subsequently, a GRNN is employed to train and learn the input variables in the data patterns, and the internal correlation among the SPNDs can be explained through the adaptivity of the neural network. We can obtain n sets of sub-models, where the features of the label SPND variable are related to the features of the neighboring SPNDs. By integrating n sub-models, we obtain an organic whole, which is an SPND twin model. Using the twin model, the errors between the model outputs and actual signals are calculated to achieve SPND fault detection. The model identifies outliers in the error sequence in combination with the generalized extreme studentized deviate (ESD) statistical test [42], which provides rapid SPND fault detection results. A fault tolerance strategy should be introduced, the foundation of which is data recovery for fault variables in response to excessive fault variables that result in the failure of fault detection. Fault signals are replaced with normal values through constant troubleshooting, data substitution, and data validation, and the performance of the twin model is recovered. When all faulty SPND are successfully identified, the detection results can assist in diagnostic decisions that can be made to maintain real detector assemblies.

A. Generalized regression neural network

To deal with sample data comprising complicated multidimensional variables, prior research concentrated on PCA, clustering, and Kalman filter methods to perform signal analysis of the SPND unit. These techniques can be used to rapidly establish models for axial SPNDs in the same detector assembly. In this study, we aimed to analyze the spatial correlation between the radially distributed SPND variables simultaneously in the plane of the reactor core. The afore-

mentioned technique is not appropriate for large-scale and nonlinear data feature mining; however, the latest neural network algorithms that an distribute information among neurons have significant robustness and can quickly analyze complex nonlinear relationships. As a typical radial basis neural network model based on nonlinear regression theory, GRNN can process high-dimensional data and mine the mutual effects among multiple SPND current features because of its capabilities of nonlinear mapping and high learning speed. Unlike other types of artificial neural networks, GRNN have straightforward structures and training processes. Therefore, we used GRNN as the constituent architecture of the SPND twin model. As shown in Fig. 4, the GRNN is composed of the input, pattern, summation, and output layers. The input and output vectors of the corresponding network are $X = [x_1, x_2, ..., x_{n-1}]^T$ and $Y = [y_1, y_2, ..., y_k]^T$, n-1 and k are the dimensions of X and Y respectively. The number of neurons in the input layer is equal to the dimensions of the input vector, and each neuron is a simple distribution unit that directly transmits the input to the pattern layer. The pattern layer is a radial base layer, whose number of neurons is equal to the number of learning samples, n-1. The neuron transfer function P_i is typically a Gaussian function and can be written as

$$P_i = exp[-(X - X_i)^T(X - X_i)/2\sigma^2], \ \ i = 1, 2, ..., n-1 \tag{1}$$

where X_i is the training sample corresponding to the i-th neuron, T is the transpose of the matrix, and σ is a smoothing factor. The smaller σ is, the stronger is the approximation ability of P_i for the samples.

There are two types of neuronal calculation formulas in the summation layer. One is to sum the outputs of all the neurons in the pattern layer. The connection weight between each neuron and the pattern layer is set to one. The transfer function can be expressed as

$$S_R = \sum_{i=1}^{m} P_i \tag{2}$$

The other type of calculation formula is to sum the outputs of all neurons in the pattern layer by weight. The transfer function can be described as

$$S_{Mj} = \sum_{t=1}^{m} w_{ij} P_i, \ \ j = 1, 2, ..., k \tag{3}$$

where w_{ij} represents the weight of the i-th neuron in the pattern layer connected to the j-th neuron element in the summation layer, S_{Mj} represents the summation value of the j-th neuron in the summation layer.

The output layer is calculated by dividing the values obtained using the two formulas in the summation layer baserd on the following equation:

$$y_j = \frac{S_{Mj}}{S_R} \tag{4}$$

where y_j is the output of the j-th output-layer neuron.

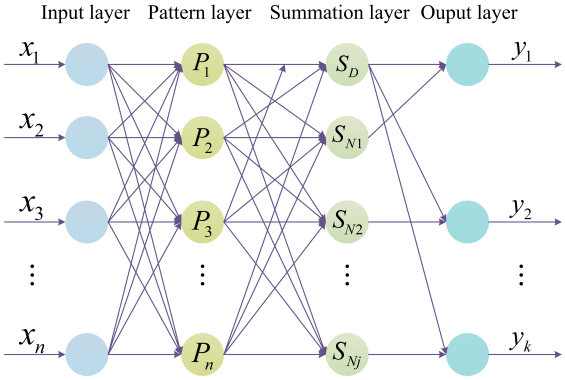

Fig. 4. Structure of the GRNN

GRNN can be applied to construct different SPND regression submodels that are integrated to form a twin model that outputs twin data.

B. Construction of the twin model

The state analysis of SPND signals with the application of DT can provide a more efficient and intelligent service for monitoring the neutron flux distribution and its rate. The premise of constructing a twin model is to extract sufficient and effective feature information from physical entities. The reactor core contains n sets of symmetrically distributed neutron flux measurement detector assemblies. Although SPNDs operate independently of each other, the multidimensional currents they produce reveal a strong cooperative link in a shared environment. The features of the nearby signals reflect the characteristics of a specific SPND signal. The relationship between SPND signals can be explained by the following equations:

$$\begin{cases} S = \{s_1, s_2, ..., s_n\} \\ D = \{d_1, d_2, ..., d_n\} \\ U = \{U_1(S), U_2(S), ..., U_n(S)\} \end{cases} \tag{5}$$

where S is the set of all SPND individuals at the same height in the reactor core, D is the set of sample values for each variable in S, and U is the set used to denote the correlations between the variables. $U_i(S)$ describes how the signal characteristics of any variable in S are collectively represented by the remanent surrounding variables. As seen in Fig. 5, the reference network $U_i(S)$ is expressed as the connectivity between the label variable and other variables. The data of the label variable can be twinned by analyzing the network of relationships among the variables. By studying the characteristics of the associated $\{s_1, s_2, ..., s_{n-1}\}$, the inherent information of the label variables can be obtained. Thus, each variable in S can also be collectively described by the others. The twin model is built based on relationship networks, and GRNN is used to construct specific submodels to form a

twin body. By dividing the set D, the n-1-dimensional variables are the features I_i and the remaining single variable is the training label T_i. After an alternate division of n groups, the data patterns between I_i and T_i are expressed as follows.

$$(I_i|T_i) = \left[\begin{array}{ccccccc} d_1 & d_2 & d_3 & \cdots & d_{n-2} & d_{n-1} & d_n \\ d_1 & d_2 & d_3 & \cdots & d_{n-2} & d_n & d_{n-1} \\ d_1 & d_2 & d_3 & \cdots & d_{n-1} & d_n & d_{n-2} \\ \vdots & \vdots & \vdots & \ddots & \vdots & \vdots & \vdots \\ d_1 & d_3 & d_4 & \cdots & d_{n-1} & d_n & d_2 \\ d_2 & d_3 & d_4 & \cdots & d_{n-1} & d_n & d_1 \end{array}\right] \tag{6}$$

The division result contains n rows of data patterns, and each dimensional variable of SPND signals in set D is designated as a label for its corresponding data pattern. For instance, SPND s_n is identified as the label of the first data pattern. Similarly, SPND s_i is considered as the label of the (n+1-i)-th data pattern. To thoroughly explore the correlation between any target variable and the remaining variables in each pattern, GRNN was utilized to train the submodels to learn the state relationships between SPND features and labels. Subsequently, n groups of submodels were built after repeated training. An integrated organism M is combined as follows:

$$M = \{M_1, M_2, ..., M_n\} \tag{7}$$

where M_i represents the trained GRNN submodels for different data patterns. After learning the algorithm, each GRNN submodel outputs the predicted value of the target SPND when its input are (n-1)-dimensional feature vectors. All submodels are combined into M, which produces n groups of estimated data and explains the commonality of signal changes in all SPND components. The real SPND signals can be twinned using these virtual values. The residual between the output results of the twin model and the real values can be calculated in the given operating scenario to determine the faulty SPNDs, and the following status assessment and potential fault tolerance can then be performed.

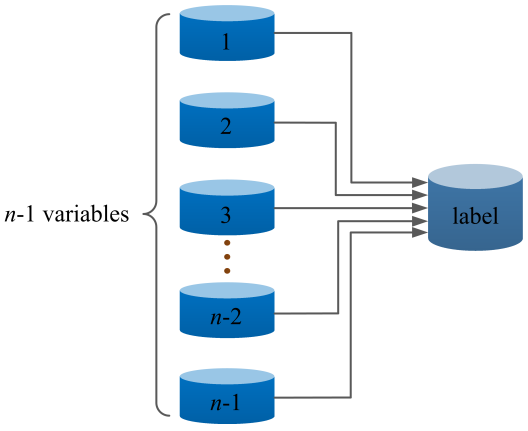

Fig. 5. The network of relationship $U_i(S)$

C. Fault detection and tolerance

Measuring the residual between the outputs of the twin model and the actual values allows us to ascertain whether faults exist in the detector assemblies. Statistical tests can generally be used to determine the deviation points in a residual sequence. Traditional statistical techniques are sensitive to the presence of outliers because inaccurate data points can distort the mean and standard deviation of a data sequence. In this section, ESD was employed to detect possible outliers in the residual sequence and discriminate the fault from the original signals. ESD can maintain a good elimination effect when several anomalies exist concurrently in the data. We assumed that outliers exist in the residual sequence. The maximum number of outliers was predetermined as r, and r rounds of separate tests were performed by calculating the variable of the statistical test, the formula of which is as follows:

$$R_i = \max \frac{|E_i - \hat{E}|}{z} \tag{8}$$

where E_i is an observed point and $\hat{E}$ and z denote the sample mean and standard deviation, respectively. The observed point that maximizes $|E_i - \hat{E}|$ and deviates the most from the mean should be located and eliminated during the calculation. The aforementioned statistic is then recalculated using the remaining n-1 observed points. The process is repeated until r observed points have been removed, resulting in the obtained r test statistics R_1, R_2, ... , R_r. Corresponding to the r test statistics, r critical values are calculated as follows:

$$\lambda_i = \frac{(n-i)t_{p,n-i-1}}{\sqrt{(n-i+1+t^2_{p,n-i})(n-i+1)}} \tag{9}$$

where $t_{p,v}$ represents the 100p percentage points from the t distribution with v degrees of freedom and $p = 1 - \frac{\alpha}{2(n-i+1)}$. α denotes the test confidence level. The number of outliers is determined by finding the largest i such that $R_i > \lambda_i$, and thus, the initial hypothesis can be true.

As mentioned above, the simultaneous failures of excessive SPNDs in detector assemblies can lead to anomalously measured data, which cannot accurately represent the actual operational status of the system. A judgment based on fault signals will cause the system to fail to reach its normal operating condition and even cause personnel to misoperate. The capacity of the twin model to perform an effective analysis suffers because of the disordered input, and the reliability and validity of the detection results cannot be demonstrated by the residual information calculated from a broken model. For the CNFMS to be dependable and secure, the fault detection function must be rehabilitated. In this case, we introduce an efficient fault-tolerant strategy, which is implemented before multi-fault detection. The most important factor to consider when designing a fault tolerance solution is that the information that should be available to the entire system after an unexpected failure must be identical to the information that

would have been obtained if the SPNDs were not faulty. The main objective was to achieve data recovery, including troubleshooting, data substitution, and data verification.

In the presence of multiple unknown fault sources, fault troubleshooting must be performed using multidimensional data. A possible selection approach involves selecting the vector with the largest calculated residual and performing data recovery first. When executing data substitution, the values of the faulty variables should be replaced with normal signals. To improve the accuracy of the replaced data, the KNN classifier was first used to select K instance points from the historical database in the nearest neighbor of the feature variable of the fault points to form a new signal sample. The operating condition of K nearest-neighbor points was the closest to that of the fault signals, and their variable characteristics were in a division range similar to the original signal characteristics. The weighted average operation was utilized for the values of these K points, which produced the corrected signal values. Finally, the fault signal values were entirely replaced by the revised values.

After data substitution, the Jensen–Shannon (JS) divergence [43] was employed to confirm the modified data and guarantee the consistency of the replacement. It can describe the differences between the probability distributions of variables, which perform well in the similarity measurement. For the two probability distributions, the interval value of the JS divergence is $[0, 1]$. The two distributions are more similar and vice versa as the value decreases. The degree of JS divergence can be used to fully evaluate the suitability of the modified data. Repeating the preceding steps for a multi-fault sample can reduce the number of faulty SPNDs after recovery until the detection results are satisfactory. When the satisfied sample is input into the twin model, the output is stable and controlled within a small error. In this case, the previous fault-detection approach is adequate and fault tolerance is no longer required.

IV. RESULTS AND DISCUSSION

In this section, the proposed method was evaluated using historical monitoring data collected from in-core detector assemblies in a third-generation pressurized water reactor. To build a reliable SPND twin model, a sufficient number of measurement datasets must be known in advance. The variables of the 44-dimensional SPND signals, which were distributed radially in a certain layer, were considered as experimental objects in this study. To improve the generalization of the twin model, training data for the twin model were derived from the reactor shutdown stage. As shown in Fig. 6, with the insertion of control rods, the power of the reactor core gradually decreased from 100% FP to 0% FP, and all the currents of SPNDs decreased. The data for the test set were derived from SPNDs during steady operation.

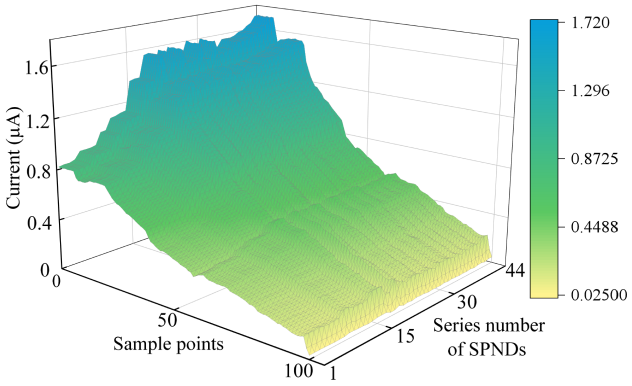

Fig. 6. SPND signals during shutdown

A. Performance of the twin model

With the continuous reduction in neutron flux during shutdown, the number of neutrons captured by the emitter decreased, resulting in a proportional decrease in the currents generated by the 44 SPNDs. To extract valuable information from physical SPNDs under different power levels and build a twin model based on it, submodels for 44 dimensional signal variables were executed. First, the training set was segmented round after round, and 44 groups of data patterns with several feature variables I_i and label variable T_i were obtained as follows:

$$(I_i|T_i) = \left[\begin{array}{cccccc|c} d_1 & d_2 & d_3 & \cdots & d_{42} & d_{43} & d_{44} \\ d_1 & d_2 & d_3 & \cdots & d_{42} & d_{44} & d_{43} \\ d_1 & d_2 & d_3 & \cdots & d_{43} & d_{44} & d_{42} \\ \vdots & \vdots & \vdots & \ddots & \vdots & \vdots & \vdots \\ d_1 & d_3 & d_4 & \cdots & d_{43} & d_{44} & d_2 \\ d_2 & d_3 & d_4 & \cdots & d_{43} & d_{44} & d_1 \end{array}\right] \tag{10}$$

Each data pattern in $(I_i|T_i)$ was input into GRNN for the model to learn the correlation between signal variables, and the 44 submodels were well-trained. The superiority of GRNN over the other models is ascribed to the convenience of its parameter setting. The performance of GRNN can only be changed by setting the smoothness factor σ in the kernel function. To improve the accuracy of the model, the root mean square error (RMSE) was employed as the loss function to optimize the value of σ for the submodels. Twenty percent of the training set was selected as the verification set and a cross-verification approach was used to obtain accurate parameter optimization results. As shown in Table 1, each submodel obtained the minimum RMSE with the corresponding setting of the optimal σ. The optimized parameters helped improve the performance of the twin model in the verification set.

To demonstrate the superiority of GRNN in modeling more clearly, we compared the proposed method with several typical approaches, including convolutional neural networks (CNN), multilayer perceptron (MLP), extreme gradient boosting (XGB), decision tree (DT), SVM, and Bayesian

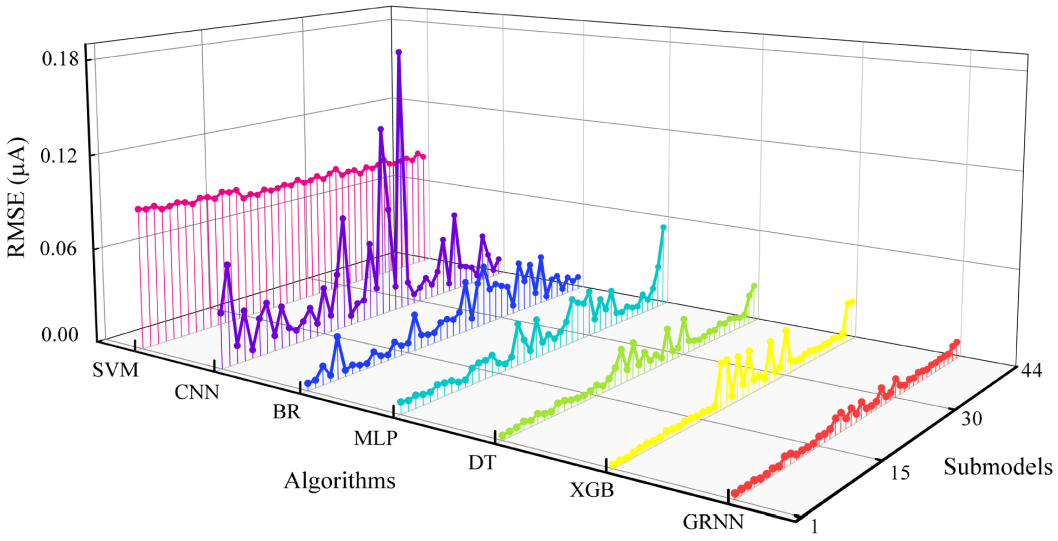

Fig. 7. Prediction errors of different algorithm-based models

ridge (BR). All methods were implemented using the same data samples from the test set to compare the output accuracies. As shown in Fig. 7, the twin model formed by GRNN had the lowest RMSE between the model outputs and actual signal values. DT and XGBoost-based models, as common tree regression algorithms, had slightly larger errors than the GRNN-based model, which can easily overfit SPND signals and reduce precision. The learning abilities of the CNN and MLP models for SPND signal features were poorer than that of the GRNN model. These models are suitable for dominant feature extraction but tend to ignore the correlation between the part and whole. SVR- and BR-based models are appropriate for handling small samples instead of analyzing larger multi-dimensional signals. Compared to typical machine learning algorithms, the twin model established based on GRNN can extract rich feature information from isolated time-varying data with lower errors and higher prediction ability. In the subsequent fault detection phase, the errors between the model outputs and actual signals can be used to determine the fault location. The estimated values of the twin model can help improve the in-core power measurement by avoiding interference from fault information.

B. Fault detection results under different conditions

The novel contribution of this study is the accurate identification of faulty SPNDs in numerous assemblies using a twin model. The signal characteristics analyzed by the twin model can help examine the fault characteristics. In this section, single- and multi-point SPND fault signals were simulated through experiments to determine the effectiveness of fault detection under different conditions. The faulty SPND signals of diverse measurement channels were simulated by adding different percentages of bias to the normal signals based on the original operating conditions.

For single-point fault detection, as shown in Fig. 8, the deviation between the output of the twin model and the actual normal value is very small before introducing faults into the test set, and the data fit well. In the simulation, a bias of 50% of the normal signal value was introduced into SPND#12 at a time point after the normal signal. In this case, the twin model could maintain a normal output, but the failure of SPND#12 caused the calculated RMSE to fluctuate significantly at this point. The results of the ESD test show that the RMSE of the 12th point deviates the most, which confirms the existence of a faulty SPND#12.

In reality, complex and changeable interference factors usually cause fault signals to vary. Different types of common fault behaviors mainly include bias, precision degradation, and complete failure, the states of which are abnormal owing to the influence of external environmental factors. The deviation in the signals also varies at the same power level that is used to measure the extent of the magnitude of failures. Experiments (15 groups $\times$ 130 rounds) were conducted to compare the fault-detection efficiency under different fault types and deviation rates. The mean accuracy, an evaluation index, is the proportion of the number of successful detections in each group of experiments to the total number of experiments. Table 2 provides the calculation results for fault detection accuracy. Except for the detection accuracy of 99.23% in "5% drifting", the mean accuracies of other cases were 100%, indating that the fault variables identified by the ESD test from errors are consistent with the actual faulty SPNDs. Therefore,

Table 1. Parameter optimization results of the 44 submodels

Submodel	σ value	RMSE (μA)	Submodel	σ value	RMSE (μA)	Submodel	σ value	RMSE (μA)	Submodel	σ value	RMSE (μA)
M_1	0.3	0.0100	M_{12}	0.13	0.0024	M_{23}	0.32	0.0110	M_{34}	0.05	0.0023
M_2	0.09	0.0020	M_{13}	0.07	0.0022	M_{24}	0.49	0.0244	M_{35}	0.02	0.0023
M_3	0.23	0.0069	M_{14}	0.14	0.0029	M_{25}	0.14	0.0029	M_{36}	0.17	0.0043
M_4	0.22	0.0065	M_{15}	0.33	0.0115	M_{26}	0.44	0.0193	M_{37}	0.07	0.0022
M_5	0.34	0.0121	M_{16}	0.02	0.0023	M_{27}	0.36	0.0133	M_{38}	0.13	0.0024
M_6	0.16	0.0038	M_{17}	0.42	0.0176	M_{28}	0.35	0.0127	M_{39}	0.05	0.0023
M_7	0.06	0.0023	M_{18}	0.48	0.0233	M_{29}	0.48	0.0233	M_{40}	0.03	0.0100
M_8	0.12	0.0021	M_{19}	0.05	0.0023	M_{30}	0.25	0.0078	M_{41}	0.32	0.0110
M_9	0.02	0.0023	M_{20}	0.21	0.0061	M_{31}	0.2	0.0057	M_{42}	0.22	0.0065
M_{10}	0.44	0.0193	M_{21}	0.38	0.0146	M_{32}	0.22	0.0065	M_{43}	0.11	0.0019
M_{11}	0.45	0.0202	M_{22}	0.06	0.0023	M_{33}	0.31	0.0105	M_{44}	0.14	0.0029

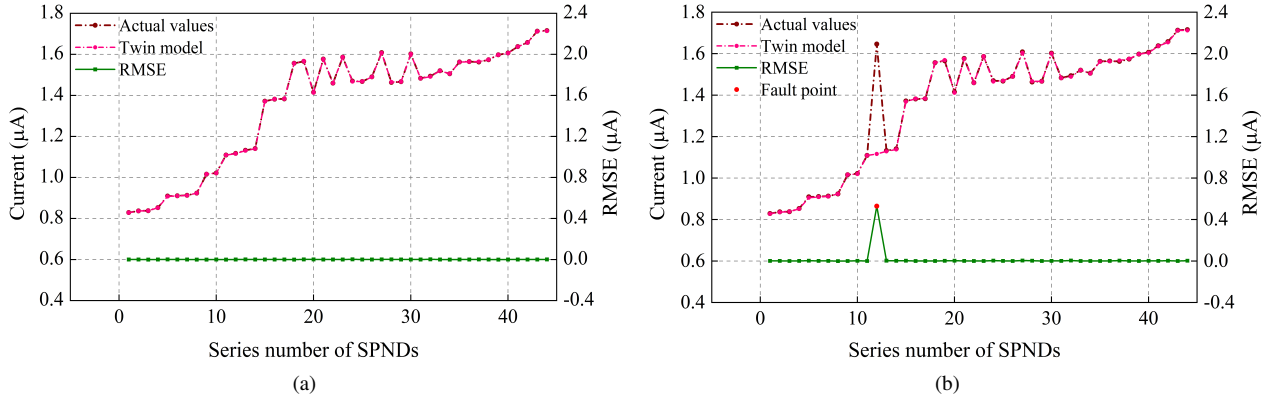

Fig. 8. Comparison of the output values of the twin model with the actual values and the RMSE of the models in the two cases

the proposed method can maintain an extremely high correct detection rate for single-point SPND faults under various conditions.

Table 2. Fault detection accuracy in various fault conditions

Fault types	Mean accuracy with different deviation rates				
	5%	20%	40%	60%	80%
Bias	100	100	100	100	100
Drifting	99.23	100	100	100	100
Precision degradation	100	100	100	100	100

Similarly, it is possible for multiple SPNDs to fail simultaneously. The method for detecting multi-point faults is the same as that for detecting single-point faults. However, this is still a challenge because multiple faulty signals can contaminate the input of the twin model, leading to rising nondeterminacy of the outputs. In this study, we analyzed the impact of the number of faulty SPNDs on the output of a twin model and the fault detection accuracy. Because the type and deviation rate of the failure size had little influence on the detection accuracy, the added simulated fault signals were random in the multi-point fault experiment (44 groups $\times$ 150 rounds). The experimental results and comparisons are shown in Fig. 9.

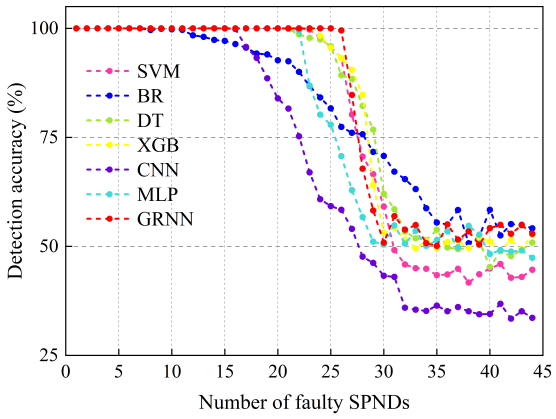

Fig. 9. Influence of the number of faults on the detection accuracy of different algorithm-based models

It was observed that the accuracy of multi-point fault de-

tection remained at 100% when the number of faulty SPNDs was less than 26. In other words, the proposed method can perform a relatively efficient detection when approximately half of the 44 SPNDs fail. As the number of failures continues to increase, the accuracy begins to gradually decrease and approaches 50%, which means that approximately half of the faulty SPNDs detected by ESD are true. Unacceptable data deviating from the normal range is the reason for the occurrence of a sharp fall. Excessive abnormal inputs strongly affect the original function of the twin model and cause it to collapse, hindering the realization of subsequent detection. With ESD test calculation, the multi-point fault detection accuracy of the models based on other algorithms declined earlier than that of GRNN-based models under identical conditions. Their accuracies decreased and slowed to different degrees with the further expansion of failure. Finally, they become more reposeful along their tails. The method proposed in this study performs well for both single- and multi-point SPND fault detection.

C. Evaluation of fault tolerance

The previous analysis proved the superiority of using the twin model to detect multiple faults. However, there is still a deficiency in dealing with excessive failures, that is, the detection accuracy decreases significantly when the number of faulty signals exceeds the upper limit. Therefore,efficient fault-tolerant solution is required to restore abnormal data. For multi-dimensional fault data points, the KNN algorithm can help search for K operating points that are closest to the faulty signal features in the historical database. On this basis, WKNN regression was employed to obtain more accurate values by assigning a greater weight to the nearest neighbors. The selection of the value of K has a significant impact on the results of the regression analysis. This is because an approximation error with a smaller K can make the model more complicated and can likely lead to overfitting, resulting in a larger estimation error. According to Fig. 10, WKNN has a lower error than KNN without weighting. When K=8, WKNN has the smallest RMSE (2.2217μA). Hence, the hyperparameter K in WKNN used in this study was set to eight.

To verify the feasibility of the fault tolerance scheme mentioned above, we selected 100 points of a continuous time sequence under the full-power platform from the test set, and random faults were introduced into SPNDs from the 25th point to the 100th point in the example. In fault-tolerant processing, data recovery is first performed for the SPND variable whose RMSE is the largest. Taking SPND#27 as an example, Fig. 11 shows that the deviation between the fault and original values is distinct (RMSE=0.0387μA), which significantly affects normal system monitoring. From the perspective of the twin model, the deviation between the predicted and original values was high (RMSE=0.0488μA), making it incapable of meeting the requirements of high-precision control. In the implementation of WKNN, the deviation distance between the regression value and the original values was the shortest (RMSE=0.0044μA), and the data recovery accuracy was enhanced compared with that of the twin model. Through data recovery, WKNN can perform more reliable correction and can maintain stable operation of the system.

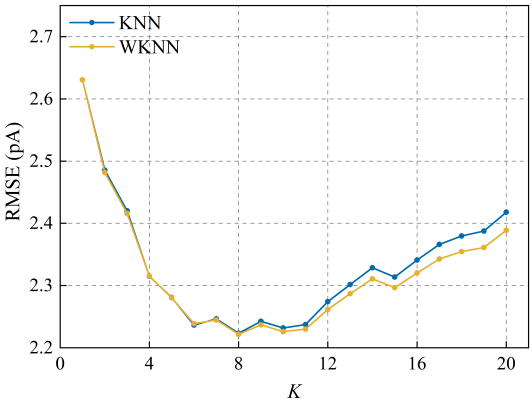

Fig. 10. Optimization of K in KNN and WKNN

For data verification, the JS divergence was employed to prove the similarity of the probability distribution of the values. After the calculation, the divergence values of the fault values, predicted values of the twin model, and regression values of WKNN with the original values were 4.3409×10^{-5}, 7.5058×10^{-7}, and 5.6829×10^{-7}, respectively. The regression values of WKNN have advantages in terms of similarity measurement which verifies the remarkably similar probability distribution and high recovery performance.

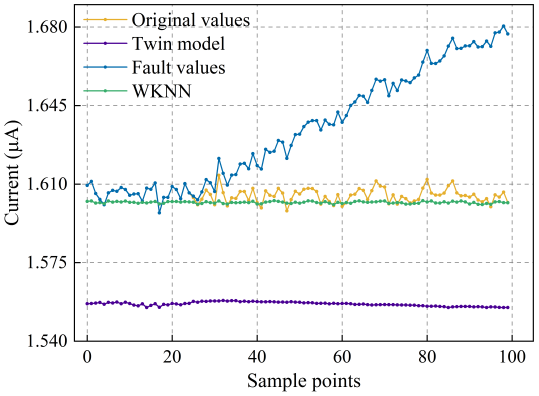

Fig. 11. Signal value of SPND#27 after data recovery

We further evaluated the performance of the fault-tolerant method on a sample filled with faulty signals. The impact of the number of recovered variables on the average RMSE of the model outputs and fault detection accuracy is illustrated in Fig. 12. In multi-point fault detection, the obtained detection accuracy with no measures for recovering data was 52.18%, which is the same as before. This is mainly attributed to the fact that the output error of the twin model is much larger than the normal range, which provides completely false knowledge and leads to the inability of the ESD test to determine

that all SPND variables have failed. As the data recovery progresses, the faulty variables are substituted by the recovered data. Subsequently, the average RMSE decreases, and the detection accuracy increases gradually. When the number of recovered variables reaches approximately 18, the accuracy increases to approximately 100%. In addition, there is no additional need to recover from other failures in this case.

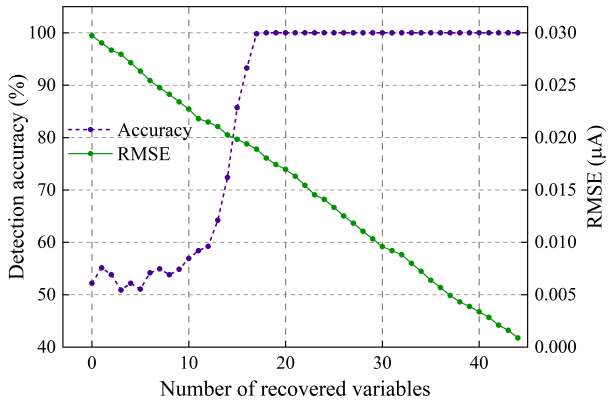

Fig. 12. Performance of fault tolerance

Finally, the effects of the fault tolerance strategy on the improvement of twin-model-based fault detection for SPNDs are discussed. As shown in Table 3, the number of faulty SPNDs was divided into five intervals in the multi-point fault detection experiment (150 groups): less than 25, 25–30, 30–35, 35–40, and more than 40. Without the introduction of fault tolerance, the mean fault detection accuracies in the five intervals were 100%, 72.23%, 53.29%, 52.91% and 53.88%. After recovering the faulty data, the number of successfully detected faulty SPNDs increased, resulting in accuracies of 100%. This change confirms that the provision of subsequent fault-tolerant measures to the twin model can efficiently enhance the detection accuracy and improve the capacity to parse the signal correlation for the model, which is sufficient for maintaining healthy monitoring of the system.

Table 3. Improvement of the fault detection accuracy with fault tolerance

Number of failure	Mean accuracy (%)	
	Before fault tolerance	After fault tolerance
≤ 25	100	100
$25 \sim 30$	72.23	100
$30 \sim 35$	53.29	100
$35 \sim 40$	52.91	100
> 40	53.88	100

V. CONCLUSION

In this study, we proposed a twin-model-based fault-detection method along with a tolerance strategy for in-core SPNDs. The twin model consists of a combination of sub-models built by GRNN, which can extract the inner correlation of multi-dimensional data through deep learning from historical SPND signals. Compared with other methods, the twin model can obtain a higher prediction precision and help improve CNFMS measurements. The fault detection phase is based on calculating the error probability distribution of the model outputs that can determine the existence of single-and multi-point faults. This technique can maintain a detection accuracy of nearly 100%. To address the problem of decreased efficiency caused by excessive failures, a fault-tolerant phase was developed with WKNN, which could search for normal signal values with the same operating conditions to replace faulty signals. Comprehensive steps, including troubleshooting, data substitution, and data verification, were conducted to achieve superior the fault-tolerance performance. The experimental results show that the tolerance strategy is promising for delivering high detection quality with an accuracy of more than 99%, suggesting that the proposed method can be considered adoptable. Furthermore, our work can be extended to other layers of in-core detector assemblies to achieve holistic condition-based maintenance of the monitoring system.

[1] M. Nakamichi, Y. Nagao, C. Yamamura, *et al.*, Characterization of hybrid self-powered neutron detector under neutron irradiation. Fusion. Eng. Des. **51-52**, 837–841 (2000). doi: 10.1016/S0920-3796(00)00452-X

[2] W. Xu, J. Li, H. xie, *et al.*, Conceptual design and safety characteristics of a new multi-mission high flux research reactor. Nucl. Sci. Tech. **34**, 34 (2023). doi: 10.1007/s41365-023-01191-6

[3] X. J. Peng, Q. Li, K. Wang, Fault detection and isolation for self powered neutron detectors based on principal component analysis. Ann. Nucl. Energy. **85**, 213–219 (2015). doi: 10.1016/j.anucene.2015.05.016

[4] K. Moshkbar-Bakhshayesh, M. B. Ghofran, Transient identification in nuclear power plants: A review. Prog. Nucl. Energy. **67**, 23–32 (2019). doi: 10.1016/j.pnucene.2013.03.017

[5] J. Ling, G. J. Liu, J. L. Li, *et al*., Fault prediction method for nuclear power machinery based on bayesian ppca recurrent neural network model. Nucl. Sci. Tech. **31**, 8 (2020). doi: 10.1007/s41365-020-00792-9

[6] P. Li, J. R. Chu, R. Han, Research on the screening method of predictive maintenance monitoring equipment in nuclear power plant. PHM-BESANCON. 128–131 (2020). doi: 10.1109/PHM-Besancon49106.2020.00027

[7] J. Hui, J. Yuan, Kalman filter, particle filter, and extended state observer for linear state estimation under perturbation (or noise) of mhtgr. Prog. Nucl. Energy. **148**, 104231 (2022). doi: 10.1016/j.pnucene.2022.104231

[8] S. Gautam, P. K. Tamboli, K. Roy, *et al*., Sensors incipient fault detection and isolation of nuclear power plant using extended kalman filter and kullback-leibler divergence. Isa. T. **92**, 180–190 (2019). doi: 10.1016/j.isatra.2019.02.011

[9] J. Hui, J. Yuan, Chattering-free higher order sliding mode controller with a high-gain observer for the load following of a pressurized water reactor. Energy. **223**, 120066 (2021). doi: 10.1016/j.energy.2021.120066

[10] Q. Gan, B. Wu, J. Song, Rapid parameter-based and visual Monte Carlo modeling method of fission reactor core. Nucl. Tech. **39**, 1–7 (2016).

[11] J. Hui, J. Yuan, Load following control of a pressurized water reactor via finite-time super-twisting sliding mode and extended state observer techniques. Energy. **241**, 122836 (2022). doi: 10.1016/j.energy.2021.122836

[12] J. Chen, Z. S. Liu, H. Jiang, *et al*., Anomaly detection of control rod drive mechanism using long short-term memory-based autoencoder and extreme gradient boosting. Nucl. Sci. Tech. **33**, 127 (2022). doi: 10.1007/s41365-022-01111-0

[13] Y. Zhao, F. Di. Maio, E. Zio, *et al*., Optimization of a dynamic uncertain causality graph for fault diagnosis in nuclear power plant. Nucl. Sci. Tech. **28**, 34 (2017). doi: 10.1007/s41365-017-0184-0

[14] W. Q. Lin, X. R. Miao, J. Chen, *et al*., Forecasting thermal parameters for ultra-high voltage transformers using long- and short-term time-series network with conditional mutual information. Iet. Electr Power App. **16**, 548–564 (2022). doi: 10.1049/elp2.12175

[15] S. Mandal, B. Santhi, S. Sridhar, *et al*., Sensor fault detection in nuclear power plants using symbolic dynamic filter. Ann. Nucl. Energy. **134**, 390–400 (2019). doi: 10.1016/j.anucene.2019.07.036

[16] V. S. Yellapu, V. Vajpayee, A. P. Tiwari, Online fault detection and isolation in advanced heavy water reactor using multiscale principal component analysis. Ieee. T. Nucl. Sci. **66**, 1790–1803 (2019). doi: 10.1109/TNS.2019.2919414

[17] V. S. Yellapu, W. D. Zhang, V. Vajpayee, *et al*., A multiscale data reconciliation approach for sensor fault detection. Prog. Nucl. Energy. **135**, 103707 (2021). doi: 10.1016/j.pnucene.2021.103707

[18] W. Li, M. Peng, Q. Wang, Fault identification in pca method during sensor condition monitoring in a nuclear power plant. Ann. Nucl. Energy. **121**, 135–145 (2018). doi: 10.1016/j.anucene.2018.07.027

[19] S. Chatterjee, S. K. Surwase, M. Bhushan, *et al*., Cluster statistics based normalization for online fault diagnosis of self-powered neutron detectors. ICICIC. (2017).

[20] Y. Yu, M. jun Peng, H. Wang, *et al*., Improved pca model for multiple fault detection, isolation and reconstruction of sensors in nuclear power plant. Ann. Nucl. Energy. **148**, 107662 (2020). doi: 10.1016/j.anucene.2020.107662

[21] N. S. Rao, C. Greulich, P. Ramuhalli, *et al*., Estimation of sensor measurement errors in reactor coolant systems using multi-sensor fusion. Nucl. Eng. Des. **375**, 111024 (2021). doi: 10.1016/j.nucengdes.2020.111024

[22] J. J. Wang, L. K. Ye, R. X. Gao, *et al*., Digital twin for rotating machinery fault diagnosis in smart manufacturing. Int. J. Prod. Res. **57**, 3920–3934 (2019). doi: 10.1080/00207543.2018.1552032

[23] K. Guo, X. Wan, L. L. Liu, *et al*., Fault diagnosis of intelligent production line based on digital twin and improved random forest. Appl. Sci-Basel. **11**, 7733 (2021). doi: 10.3390/app11167733

[24] L. Y. Lin, P. Athe, P. Rouxelin, *et al*., Digital-twin-based improvements to diagnosis, prognosis, strategy assessment, and discrepancy checking in a nearly autonomous management and control system. Ann. Nucl. Energy. **166**, 108715 (2022). doi: 10.1016/j.anucene.2021.108715

[25] Y. Cai, B. Starly, P. Cohen, *et al*., Sensor data and information fusion to construct digital-twins virtual machine tools for cyber-physical manufacturing. NAMRC. **10**, 1031–1042 (2017). doi: 10.1016/j.promfg.2017.07.094

[26] R. M. Ayo-Imoru, A. A. Ali, P. N. Bokoro, *et al*., An enhanced fault diagnosis in nuclear power plants for a digital twin framework. ICECET. 2072–2077 (2021). doi: 10.1109/ICECET52533.2021.9698715

[27] W. Q. Liu, L. F. Han, L. Huang, *et al*., TMSR-SF0 data monitoring and visualization scheme based on digital twin. Nucl. Tech. **45**, 83–90 (2022).

[28] B. Kochunas, X. Huan, Digital twin concepts with uncertainty for nuclear power applications. Energies. **14**, 4235 (2021). doi: 10.3390/en14144235

[29] A. C. F. Guimaraes, C. M. F. Lapa, M. D. Moreira, Fuzzy methodology applied to probabilistic safety assessment for digital system in nuclear power plants. Nucl. Eng. Des. **241**, 3967–3976 (2011). doi: 10.1016/j.nucengdes.2011.06.044

[30] M. Hu, F. Kong, D. Yu, *et al*., Key technology and prospects of digital twin in field of advanced nuclear energy. Power. Syst. Tech. **45**, 2514–2522 (2021). doi: 1000-3673(2021)45:7<2514:SZLSZX>2.0.TX;2-2

[31] W. Wang, M. Liu, J. Li, Research and realization of virtual-real control of robot system for off-heap detector assisted installation based on digital twin. Ieee. J. Radio. Freq. Ident. **6**, 810–814 (2022). doi: 10.1109/JRFID.2022.3209715

[32] H. Gong, S. Cheng, Z. Chen, *et al*., Data-enabled physics-informed machine learning for reduced-order modeling digital twin: Application to nuclear reactor physics. Nucl. Sci. Eng. **196**, 668–693 (2022). doi: 10.1080/00295639.2021.2014752

[33] S. A. Cancemi, R. Lo Frano, The application of machine learning for on-line monitoring nuclear power plant performance. NENE. 505 (2021).

[34] W. Zhang, G. Wang, X. Zhu, *et al*., Digital twin-based optimization design method for aerospace electric thruster. J. Astronaut. **43**, 518–527 (2022). doi: 1000-1328(2022)43:4<518:JYSZLS>2.0.TX;2-P

[35] J. Y. Li, H. Xia, S. Y. Cheng, Study on sensor with mechanical properties in nuclear power plant with application of bp neural

network to fault tolerant control. MEE. **644**, 56–89 (2013). doi: 10.4028/www.scientific.net/AMR.644.56

[36] M. C. Kim, J. Seo, W. Jung, *et al*., Evaluation of effectiveness of fault-tolerant techniques in a digital instrumentation and control system with a fault injection experiment. Nucl. Eng. Tech. **51**, 692–701 (2019). doi: 10.1016/j.net.2018.11.012

[37] J. Hui, J. Yuan, Neural network-based adaptive fault-tolerant control for load following of a mhtgr with prescribed performance and crdm faults. Energy. **257**, 124663 (2022). doi: 10.1016/j.energy.2022.124663

[38] C. Li, R. Yu, W. Yu, *et al*., Fault-tolerant control system for once-through steam generator based on reinforcement learning algorithm. Nucl. Eng. Tech. **54**, 3283–3292 (2022). doi: 10.1016/j.net.2022.04.014

[39] P. H. Rangegowda, S. C. Patwardhan, S. Mukhopadhyay, Fault tolerant control of a nuclear steam generator in the presence of sensor biases. ACODS. **53**, 579–584 (2020). doi: 10.1016/j.ifacol.2020.06.097

[40] R. Behkam, H. Karami, M. S. Naderi, *et al*., Generalized regression neural network application for fault type detection in distribution transformer windings considering statistical indices. Compel. **41**, 381–409 (2022). doi: 10.1108/COMPEL-06-2021-0199

[41] C. Zhang, X. W. Gao, Y. Li, *et al*., Fault detection strategy based on weighted distance of k nearest neighbors for semiconductor manufacturing processes. Ieee. T. Semiconduct. M. **32**, 75–81 (2019). doi: 10.1109/TSM.2018.2857818

[42] A. Karlstrom, L. Johansson, J. Hill, On the modeling of tensile index from larger data sets. Nordic Pulp Paper Research Journal. **34**, 289–303 (2019). doi: 10.1515/npprj-2018-0019

[43] Y. Wang, Y. Wang, J. Deng, *et al*., Recommendation algorithm based on jensen-shannon divergence. Comput. Sci. **46**, 210–214 (2019). doi: 1002-137X(2019)46:2<210:RHJSSD>2.0.TX;2-6